Systematic study of the isotopic behavior of the fusion cross section at energies near and below the fusion barrier using the proximity formalism

O. N. Ghodsi and A. Moradi

Sciences Faculty, Department of Physics, University of Mazandaran, P.O. Box 47415-416, Babolsar, Iran
and Sciences Faculty, Physics Group, Payame Noor University, P.O. Box 19395-4697, Tehran, Iran

(Received 9 February 2014; revised manuscript received 15 May 2014; published 27 June 2014)

The isotopic behavior of the fusion cross sections and barrier curvature at energies near and below the barrier are explored using the proximity formalism. For this purpose, various versions of the proximity potentials are used to calculate the nuclear part of the interaction potential. Our study has been restricted to the isotopic systems which obey the condition of $0.5 \leqslant N/Z \leqslant 1.6$ for their compound nuclei. The obtained results show that the barrier curvature and the fusion cross section follow a similar behavior at near- and below-barrier energies. In fact, these quantities decrease nonlinearly (second order) with the addition of a neutron. In the present study, the energy dependence of the fusion cross sections is also discussed for the considered isotopic systems.

DOI: 10.1103/PhysRevC.89.064612 PACS number(s): 25.70.Jj, 24.10.−i

I. INTRODUCTION

The systematic study of the isotopic dependence of the barrier characteristics such as barrier height (V_b) and position (R_b) versus the N/Z ratio, where N (Z) is the neutron (proton) number of the compound nucleus, has received a lot of attention in recent years [1–6]. So far, those investigations have been carried out by using different models [7–15] such as the Skyrme energy density model, and the Ngo and Ngo, Christensen and Winther, Bass, and Denisov potentials. The obtained results of the previous studies show that by adding a neutron, the barrier height decreases linearly whereas the barrier position increases linearly for proton- or neutron-rich systems. But in the whole range of N/Z the ratio (both proton- and neutron-rich systems), the investigations confirm a nonlinear dependence for these barrier characteristics [1–6]. Another important issue of the isotopic studies is the analysis of the isotopic behavior of the fusion cross sections versus the N/Z ratio. It must be noted that the isotopic trend of the fusion cross sections is restricted to the above-barrier energies in all of the mentioned studies. It is indicated that the fusion cross sections increase linearly for both proton- and neutron-rich nuclei [1–6]. It is well known that by adding a neutron to each fusion system, the attractive nuclear force increases. Therefore, one expects increasing and decreasing trends for calculated values of the barrier positions and the barrier heights, respectively. Moreover since the fusion cross section is directly dependent on these mentioned parameters, it is predictable that this quantity has an increasing trend, as a function of N/Z ratio.

Recently, the isotopic behavior of fusion cross sections and barrier characteristics were analyzed for proton- and neutron-rich nuclei [6]. In that study, 125 fusion reactions were selected under condition $0.5 \leqslant N/Z \leqslant 1.6$ for their compound nuclei. The obtained results revealed the linear trend of σ_{fus} versus the ratio of N/Z at above-barrier energies.

In the present work, the analysis of the isotopic behavior of the fusion cross sections is extended to energies near and below the barrier. Our motivation to choose this issue is that the fusion reactions take place by quantum tunneling at these energies. Because of this different procedure, one may expect a different isotopic trend for fusion cross sections at these energies compared to the above-barrier ones. In this study, the nuclear part of the interaction potential is calculated using various versions of the proximity formalism such as AW 95 [16], Bass 80 [17,18], Denisov DP [19], and Prox.2010 [20] potential models. Moreover, the Wong model [21] is employed to calculate the theoretical values of the fusion cross sections.

The present paper is organized as follows. In Sec. II, we discuss the theoretical framework used to calculate the nuclear potential and fusion cross section. The analysis of isotopic behavior of cross sections at near- and below-barrier energies is presented in Sec. III and a review of our important conclusions is discussed in Sec. IV.

II. THEORETICAL FORMALISM

It is well accepted that the interacting potential between a colliding pair is a key factor in the calculation of fusion cross sections. So first we give a brief review of how one can calculate this potential. The total potential can be considered as a sum of nuclear and Coulomb parts:

$$V_{\text{tot}}(r) = V_N(r) + V_C(r) = V_N(r) + \frac{Z_1 Z_2 e^2}{r}, \tag{1}$$

where Z_1 and Z_2 are atomic numbers of the interaction nuclei. In recent years many theoretical models have been introduced for calculating the nuclear part. One useful model for achieving this goal is the proximity formalism. Various versions of this formalism are introduced in Refs. [20,22]. In the present work, we calculate the interaction potential using proximity potentials AW 95, Bass 80, Denisov DP, and Prox.2010 which are briefly introduced as follows:

$$V_N^{\text{AW95}}(r) = -\frac{V_0}{1+\exp\left(\frac{r-R_0}{a}\right)}, \tag{2}$$

$$V_N^{\text{Bass80}}(r) = -\frac{R_1 R_2}{R_1+R_2}\Phi(s = r - R_1 - R_2), \tag{3}$$

$$V_N^{\mathrm{DenisovDP}}(r) = -1.989843\frac{R_1R_2}{R_1+R_2}\Phi(s = r - R_1 - R_2 - 2.65)\left[1 + 0.003525139\left(\frac{A_1}{A_2}+\frac{A_2}{A_1}\right)^{3/2} - 0.4113263(I_1+I_2)\right], \tag{4}$$

$$V_N^{\mathrm{Prox.2010}}(r) = 4\pi\gamma\frac{R_1R_2}{R_1+R_2}\Phi(s = r - C_1 - C_2). \tag{5}$$

Details of these formulas are more completely expressed in Refs. [16–20,22]. Also the universal functions $\Phi(s)$ are defined by Eqs. (20), (42), and (6) of Ref. [22] for Bass 80, Denisov DP, and Prox.2010 potentials, respectively. Once the total potential $V_{\mathrm{tot}}(r)$ is known, one can extract the barrier height (V_b) and barrier position (R_b) using the relation

$$\left(\frac{dV_{\mathrm{tot}}(r)}{dr}\right)_{r=R_b} = 0; \quad \left(\frac{d^2V_{\mathrm{tot}}(r)}{dr^2}\right)_{r=R_b} \leqslant 0. \tag{6}$$

When the values of V_b and R_b are determined, one can calculate the fusion cross section using the Wong model. According to this model the fusion cross section is given by

$$\sigma_{\mathrm{fus}} = \frac{\pi}{k^2}\sum_{l=0}^{l_{\max}}(2l+1)T_l(E_{\mathrm{c.m.}}), \tag{7}$$

here $k = \sqrt{(2\mu E_{\mathrm{c.m.}})/\hbar^2}$). Also μ is the reduced mass of the interacting system and $E_{\mathrm{c.m.}}$ is the center-of-mass energy. The quantum mechanical transmission probability through the potential barrier for a specified angular momentum ℓ and c.m. energy, namely, $T_\ell(E_{\mathrm{c.m.}})$, is given as follows:

$$T_\ell(E_{\mathrm{c.m.}}) = \left[1 + \exp\left(\frac{2\pi}{\hbar\omega_\ell}\right)(V_b - E_{\mathrm{c.m.}})\right]^{-1}, \tag{8}$$

where $\hbar\omega_\ell$ is the curvature of the inverted parabola. If we assume that the barrier position and width are independent of the value of ℓ, we can rewrite the definition of the fusion cross section Eq. (4) as the form

$$\sigma_{\mathrm{fus}} = \frac{10R_b^2\hbar\omega}{2E_{\mathrm{c.m.}}}\ln\left[1 + \exp\left(\frac{2\pi}{\hbar\omega}\right)(V_b - E_{\mathrm{c.m.}})\right], \tag{9}$$

here the barrier curvature in the case of $\ell = 0$ is denoted by $\hbar\omega$. It can be proved that the fusion cross section defined by Eq. (6) reduces to the following relation for subbarrier energies:

$$\sigma_{\mathrm{fus}} = \frac{10R_b^2\hbar\omega}{2E_{\mathrm{c.m.}}}\exp\left(\frac{2\pi}{\hbar\omega}\right)(V_b - E_{\mathrm{c.m.}}). \tag{10}$$

According to the Wong approach, the value of $\hbar\omega$ can be determined by [21]

$$\hbar\omega = \hbar\left[\frac{1}{\mu}\left(\frac{d^2V_{\mathrm{tot}}(r)}{dr^2}\right)_{r=R_b}\right]^{1/2}. \tag{11}$$

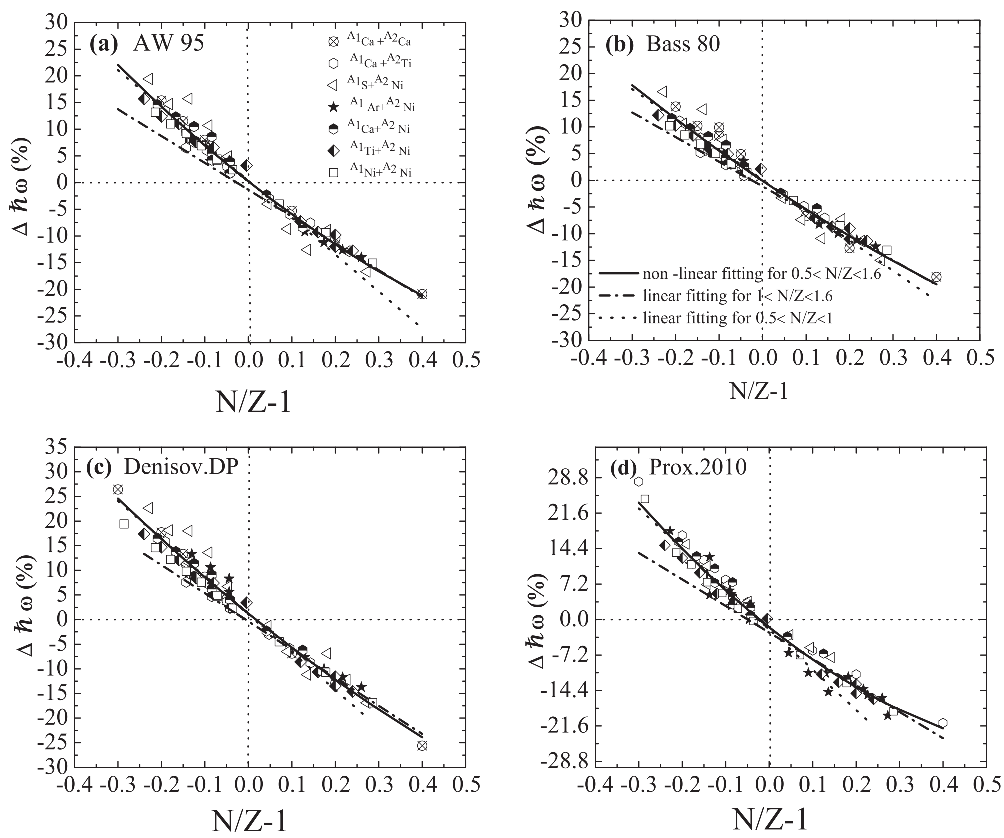

FIG. 1. Variation trend of $\hbar\omega$ as a function of $(N/Z-1)$ based on the selected potentials (a) AW 95, (b) Bass 80, (c) Denisov DP, and (d) Prox.2010. In each panel, the dotted and dash-dotted lines are related to $\Delta\hbar\omega(\%)$ values in $0.5 \leqslant N/Z \leqslant 1$ and $1 \leqslant N/Z \leqslant 1.6$ regions, respectively. The solid curves show a nonlinear fitting of the calculated values in the whole range of $0.5 \leqslant N/Z \leqslant 1.6$.

III. RESULTS AND DISCUSSION

In this study, we analyze the isotopic behavior of the barrier curvature and fusion cross section using Eqs. (10) and (11) at near- and below-barrier energies. For this purpose, we define the percentage difference of σ_{fus} and $\hbar\omega$ as follows:

$$\Delta\sigma_{\mathrm{fus}}(\%) = \frac{\sigma_{\mathrm{fus}}(E_{\mathrm{c.m.}}) - \sigma^0_{\mathrm{fus}}(E_{\mathrm{c.m.}})}{\sigma^0_{\mathrm{fus}}(E_{\mathrm{c.m.}})} \times 100, \qquad (12)$$

$$\Delta\hbar\omega(\%) = \frac{\hbar\omega - \hbar\omega^0}{\hbar\omega^0} \times 100, \qquad (13)$$

where $\sigma^0_{\mathrm{fus}}(E_{\mathrm{c.m.}})$ and $\hbar\omega^0$ are the fusion cross section and barrier curvature for $N = Z$ cases, respectively.

A. Isotopic dependence of the barrier curvature

According to Eq. (10), one can see that the fusion cross section depends on the three parameters of barrier height (V_b), barrier position (R_b), and barrier curvature ($\hbar\omega$). The isotopic trends of V_b and R_b are similar to those presented in Fig. 4 of Ref. [6]. So it is quite reasonable that we first examine the isotopic dependence of the barrier curvature. In our calculations, we initially divide the isotopic reactions into proton-rich ($0.5 \leqslant N/Z \leqslant 1$) and neutron-rich ($1 \leqslant N/Z \leqslant 1.6$) cases to examine the isotopic trends of the mentioned quantities. The calculated values of $\Delta\hbar\omega(\%)$ based on the selected proximity models are displayed in Fig. 1. It is shown that these values linearly reduce with the increase of the N/Z ratio for each of the proton- or neutron-rich regions. We employ the following formula to parametrize these trends:

TABLE I. Calculated values of the constant coefficients α_i and α_i^* (with $i = 1, 2$).

Proximity-model	α_1	α_2	α_1^*	α_2^*
AW 95	−69.13	−50.27	−64.51	27.41
Bass 80	−56.71	−46.14	−54.89	15.98
Denisov DP	−76.72	−57.16	−71.35	21.19
Prox.2010	−81.78	−53.76	−70.20	47.18

$$\Delta\hbar\omega(\%) = \alpha_1\left(\frac{N}{Z} - 1\right), \quad \text{for} \quad N/Z \leqslant 1, \qquad (14)$$

$$\Delta\hbar\omega(\%) = \alpha_2\left(\frac{N}{Z} - 1\right), \quad \text{for} \quad N/Z \geqslant 1, \qquad (15)$$

where the extracted values of the constant coefficients α_1 and α_2 are presented in Table I. In Fig. 1, the isotopic trends of $\Delta\hbar\omega(\%)$ are displayed based on the proximity potentials of AW 95, Bass 80, Denisov DP, and Prox.2010 for different colliding systems. An important result drawn from this figure is that the linear behaviors of the barrier curvatures change

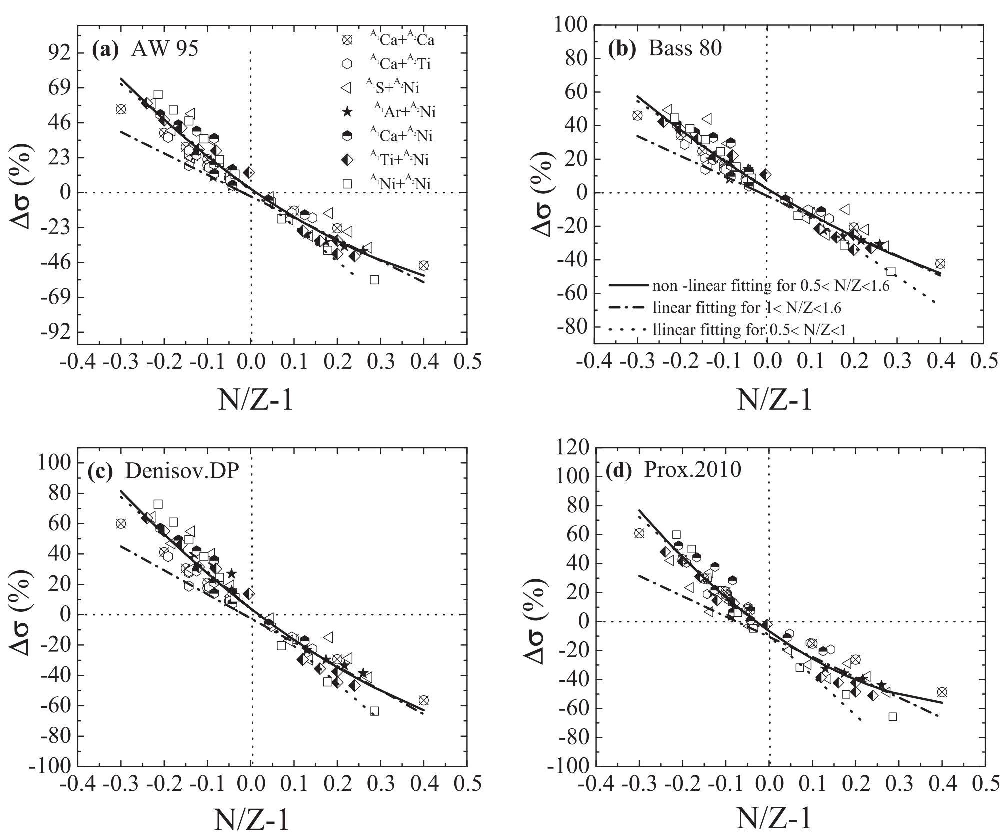

FIG. 2. Percentage difference of the fusion cross section $\Delta\sigma_{\mathrm{fus}}(\%)$ as a function of $(N/Z - 1)$ based on the potentials (a) AW 95, (b) Bass 80, (c) Denisov DP, and (d) Prox.2010 for $E_{\mathrm{c.m.}} = 0.95V_b$. The dotted and dash-dotted lines show a linear fitting of the function $\Delta\sigma_{\mathrm{fus}}(\%)$ in $0.5 \leqslant N/Z \leqslant 1$ and $1 \leqslant N/Z \leqslant 1.6$ regions, respectively. The solid curves show a non-linear fitting of the calculated values in the whole range of $0.5 \leqslant N/Z \leqslant 1.6$.

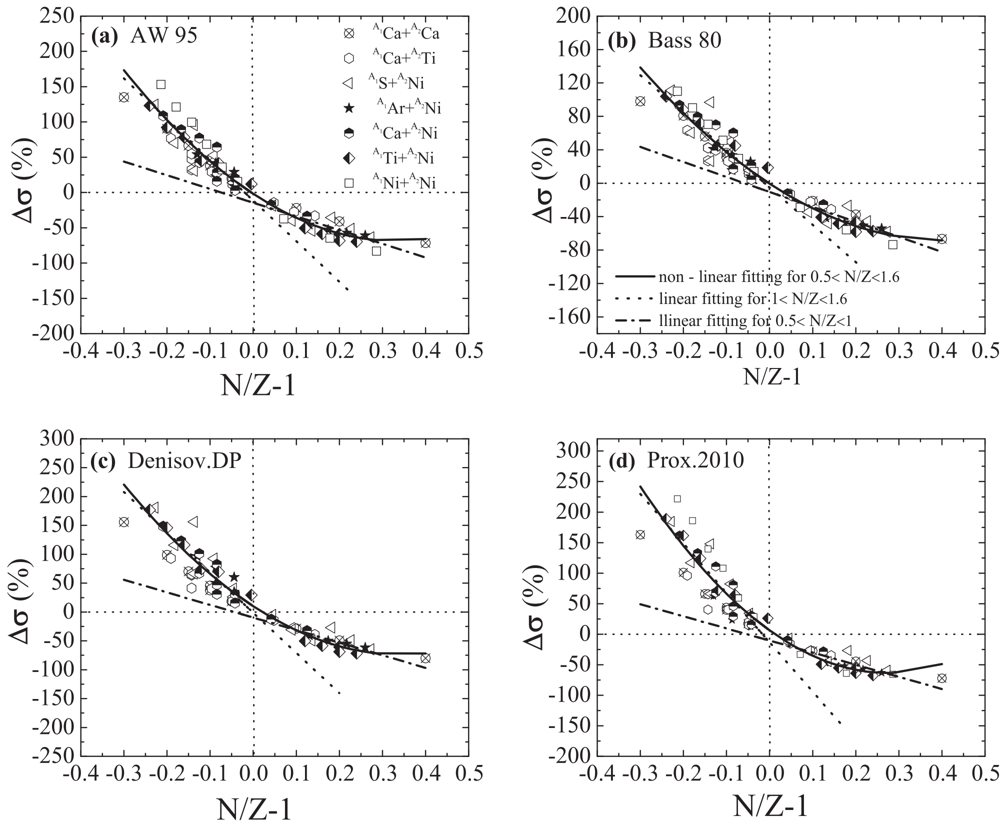

FIG. 3. Same as Fig. 2, but for $E_{\text{c.m.}} = 0.9V_b$.

nonlinearly (second-order) for all proton- and neutron-rich systems. Based on the considered potential models, these behaviors can be formulated as follows:

$$\Delta\hbar\omega(\%) = \alpha_1^*\left(\frac{N}{Z}-1\right) + \alpha_2^*\left(\frac{N}{Z}-1\right)^2. \tag{16}$$

The values of the α_1^* and α_2^* constants are listed in Table I.

B. Isotopic dependence of the fusion cross section

Like the barrier curvature, we can analyze the isotopic trend of σ_{fus} for each of the separated regions of the N/Z ratio. For this purpose, the values of $\Delta\sigma_{\text{fus}}(\%)$ have been systematically calculated at two different below-barrier energies: $E_{\text{c.m.}} = 0.9V_b$ and $E_{\text{c.m.}} = 0.95V_b$, for example. Our obtained results reveal a linear trend for these values against the ratio of N/Z in the isotopic regions $N/Z \leqslant 1$ or $N/Z \geqslant 1$, see Figs. 2 and 3. Moreover, the increase of neutrons in the considered reactions gives rise to the decrease of the calculated fusion cross sections. In the mentioned regions, one can parametrize the regular behavior of this quantity as a function of the N/Z ratio using the following relations:

$$\Delta\sigma_{\text{fus}}(\%) = \beta_1\left(\frac{N}{Z}-1\right), \quad \text{for} \quad N/Z \leqslant 1, \tag{17}$$

$$\Delta\sigma_{\text{fus}}(\%) = \beta_2\left(\frac{N}{Z}-1\right), \quad \text{for} \quad N/Z \geqslant 1, \tag{18}$$

where for selected energies of $E_{\text{c.m.}} = 0.9V_b$ and $E_{\text{c.m.}} = 0.95V_b$ the values of the constant coefficients β_1 and β_2 are listed in Table II. As a second result of Figs. 2 and 3, it can be pointed out that the isotopic behaviors of the obtained values of $\Delta\sigma_{\text{fus}}(\%)$ based on the selected proximity potentials are nonlinear (second-order) in the whole range of N/Z ratio (i.e., $0.5 \leqslant N/Z \leqslant 1.6$). We parametrize these behaviors by employing the relation

$$\Delta\sigma_{\text{fus}}(\%) = \beta_1^*\left(\frac{N}{Z}-1\right) + \beta_2^*\left(\frac{N}{Z}-1\right)^2, \tag{19}$$

TABLE II. Calculated values of the constant coefficients β_i and β_i^* (with $i = 1, 2$) for $E_{\text{c.m.}} = 0.9V_b$ and $E_{\text{c.m.}} = 0.95V_b$ energies.

Proximity-model	β_1	β_1	β_2	β_2	β_1^*	β_1^*	β_2^*	β_2^*
$E_{\text{c.m.}}$	$0.9V_b$	$0.95V_b$	$0.9V_b$	$0.95V_b$	$0.9V_b$	$0.95V_b$	$0.9V_b$	$0.95V_b$
AW 95	−576.80	−232.65	−194.20	−141.49	−402.30	−119.51	604.20	141.02
Bass 80	−447.57	−174.38	−179.51	−118.75	−333.73	−158.79	419.20	82.49
Denisov DP	−696.84	−245.43	−217.83	−157.91	−488.91	−219.93	709.15	128.21
Prox.2010	−809.40	−273.60	−198.56	−139.94	−507.96	−211.56	924.82	219.47

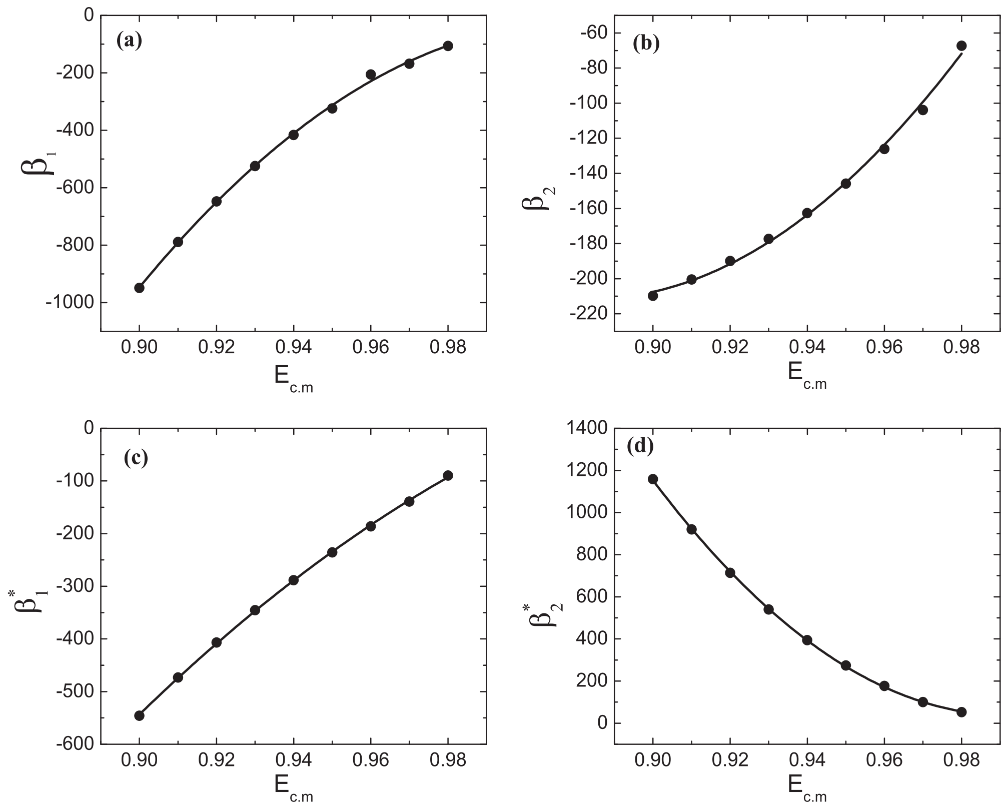

FIG. 4. Behaviors of the constant coefficients (a) β_1, (b) β_2, (c) β_1^*, and (d) β_2^* as a function of the center-of-mass energy $E_{\text{c.m.}}$. The center of mass energy is shown in units of V_b (barrier height).

where the values of the constant coefficients β_1^* and β_2^* for each of two mentioned energies are listed in Table II.

It is remarkable that the isotopic behaviors of fusion cross sections at below-barrier energies are in contrast with those obtained at above-barrier ones, see previous studies such as Refs. [1–6]. This difference is predictable because the fusion reaction of two colliding nuclei takes place through quantum tunneling at near- and below-barrier energies. Moreover by comparing the isotopic behaviors of the fusion cross section and barrier curvature, it seems that there are similar isotopic trends between these quantities at subbarrier energies.

C. Energy dependence of the fusion cross section

As we noted earlier, in the present study, the isotopic dependence of the fusion cross sections has been explored at near- and below-barrier energies $E_{\text{c.m.}} = 0.9V_b$ and $E_{\text{c.m.}} = 0.95V_b$. By comparing the obtained results in Figs. 2 and 3, one can demonstrate that the calculated values of the percentage difference of σ_{fus} depend not only on the ratio of N/Z, but also on the center-of-mass energy. Since the extracted values of coefficients β_i and β_i^* (with $i = 1,2$) change with increase of $E_{\text{c.m.}}$ in the three considered isotopic regions, such dependence can be attributed to these coefficients.

To achieve a systematic behavior of the energy dependence of the function $\Delta\sigma_{\text{fus}}(\%)$, we evaluate the values of this function at an arbitrary energy range $E_{\text{c.m.}} = 0.9V_b$ to $E_{\text{c.m.}} = 0.98V_b$. These calculations are performed for example using the Prox.2010 potential. It is shown that the extracted values of β_1 and β_2 parameters have a regular trend as a function of $E_{\text{c.m.}}$ for neutron- or proton-rich systems, see Fig. 4. By considering such extra dependence, Eqs. (17) and (18) are modified as follows:

$$\Delta\sigma_{\text{fus}}^{\text{Mod.}}(\%) = \beta_1(E_{\text{c.m.}})\left(\frac{N}{Z} - 1\right), \quad \text{for} \quad N/Z \leqslant 1, \quad (20)$$

$$\Delta\sigma_{\text{fus}}^{\text{Mod.}}(\%) = \beta_2(E_{\text{c.m.}})\left(\frac{N}{Z} - 1\right), \quad \text{for} \quad N/Z \geqslant 1, \quad (21)$$

where the energy-dependent forms of the β coefficients can be parametrized by the relation

$$\beta_i(E_{\text{c.m.}}) = \gamma_{0i} + \gamma_{1i}\, E_{\text{c.m.}} + \gamma_{2i}\, E_{\text{c.m.}}^2, \quad \text{for} \quad (i = 1,2), \quad (22)$$

where the values of the constant coefficients $\gamma_{(0,1,2)i}$ are presented in Table III.

TABLE III. Extracted values of the constant coefficients $\gamma_{(0,1,2)i}$ and $\gamma_{(0,1,2)i}^*$.

γ constants ($\times 10^6$)		γ^* constants ($\times 10^6$)	
γ_{01}	−0.0740	γ_{01}^*	−0.0218
γ_{11}	0.1462	γ_{11}^*	0.0401
γ_{21}	−0.0721	γ_{21}^*	−0.0183
γ_{02}	0.0115	γ_{02}^*	0.1301
γ_{12}	−0.0265	γ_{12}^*	−0.2623
γ_{22}	0.0150	γ_{22}^*	0.1322

It must be noted that the energy dependence of the function $\Delta\sigma_{\rm fus}(\%)$ can be considered for the full range of N/Z ratios. As a result of Fig. 4, the extracted values of β_i^* have also a regular behavior versus the center-of-mass energy in the selected energy range of $E_{\rm c.m.} = 0.9V_b$ to $0.98V_b$. By imposing such dependence in Eq. (19), the analytical form of the percentage difference of the fusion cross section is modified as follows:

$$\Delta\sigma_{\rm fus}^{\rm Mod.}(\%) = \beta_1^*(E_{\rm c.m.})\left(\frac{N}{Z} - 1\right) + \beta_2^*(E_{\rm c.m.})\left(\frac{N}{Z} - 1\right)^2, \tag{23}$$

where the energy-dependent forms of $\beta_1^*(E_{\rm c.m.})$ and $\beta_2^*(E_{\rm c.m.})$ functions are given as

$$\beta_i^*(E_{\rm c.m.}) = \gamma_{0i}^* + \gamma_{1i}^* E_{\rm c.m.} + \gamma_{2i}^* E_{\rm c.m.}^2, \quad \text{for} \quad (i = 1,2), \tag{24}$$

where the values of the constant coefficients $\gamma_{(0,1,2)i}^*$ are presented in Table III.

IV. CONCLUSION

In the present study, four versions of the proximity potential and also the Wong model are used to analyze the isotopic dependence of the barrier curvature and fusion cross section at near- and below-barrier energies. The selected fusion reactions include different isotopes systems under the condition $0.5 \leqslant N/Z \leqslant 1.6$ for their compound nuclei. Our obtained results for the three considered regions of N/Z ratio can be summarized as follows: (i) For proton- or neutron-rich systems, the calculated values of the barrier curvature and also the fusion cross section decrease linearly by adding neutrons. (ii) The reduction behavior of the considered quantities are also maintained in the whole range of $0.5 \leqslant N/Z \leqslant 1.6$ with this difference that they follow a nonlinear (second-order) trend at this range. (iii) As a result, it must be noted that the isotopic dependence of the fusion cross sections is different at below- and above-barrier energies. In fact, in the previous study, it is shown that the fusion cross sections are enhanced by increasing the N/Z ratio at above-barrier energies [6], whereas they follow a decreasing trend at near- and below-barrier energies. The most important reason for the observed difference between the isotopic behaviors of the calculated fusion cross section at these two energy ranges can be attributed to the quantum tunneling phenomenon through the Coulomb barrier which takes place at below-barrier energies. (iv) In addition to the isotopic dependence, the results of the present study reveal an energy dependence for the function of $\Delta\sigma_{\rm fus}(\%)$, see Figs. 2 and 3.

[1] R. K. Puri, M. K. Sharma, and R. K. Gupta, Eur. Phys. J. A **3**, 277 (1998).
[2] R. K. Puri and N. K. Dhiman, Eur. Phys. J. A **23**, 429 (2005).
[3] N. K. Dhiman and R. K. Puri, Acta. Phys. Pol. B **37**, 1855 (2006).
[4] I. Dutt and R. K. Puri, Phys. Rev. C **81**, 044615 (2010).
[5] O. N. Ghodsi and R. Gharaei, Eur. Phys. J. A **48**, 21 (2012).
[6] O. N. Ghodsi, R. Gharaei, and F. Lari, Phys. Rev. C **86**, 024615 (2012).
[7] D. M. Brink and N. Rowley, Nucl. Phys. A **219**, 79 (1974).
[8] D. M. Brink and Fl. Stancu, Nucl. Phys. A **243**, 175 (1975).
[9] Fl. Stancu and D. M. Brink, Nucl. Phys. A **270**, 236 (1976).
[10] D. M. Brink and Fl. Stancu, Nucl. Phys. A **299**, 321 (1978).
[11] C. Ngo, B. Tamain, M. Beiner, R. J. Lombard, D. Mas, and H. H. Deubler, Nucl. Phys. A **252**, 237 (1975).
[12] H. Ngo and Ch. Ngo, Nucl. Phys. A **348**, 140 (1980).
[13] R. K. Puri and R. K. Gupta, Phys. Rev. C **45**, 1837 (1992).
[14] R. K. Puri and R. K. Gupta, Phys. Rev. C **51**, 1568 (1995).
[15] M. K. Sharma, R. K. Puri, and R. K. Gupta, Z. Phys. A **359**, 141 (1997).
[16] A. Winther, Nucl. Phys. A **594**, 203 (1995).
[17] R. Bass, Phys. Rev. Lett. **39**, 265 (1977).
[18] R. Bass, in *Lecture Notes in Physics* (Springer, Berlin, 1980), Vol. 117, p. 281.
[19] V. Y. Denisov, Phys. Lett. B **526**, 315 (2002).
[20] I. Dutt and R. K. Puri, Phys. Rev. C **81**, 047601 (2010).
[21] C. Y. Wong, Phys. Lett. B **42**, 186 (1972); Phys. Rev. Lett. **31**, 766 (1973).
[22] I. Dutt and R. K. Puri, Phys. Rev. C **81**, 064609 (2010).